Origin of the 2450 cm^{-1} Raman bands in HOPG, single-wall and double-wall carbon nanotubes

T. Shimada [a], T. Sugai [a], C. Fantini [b], M. Souza [b], L.G. Cançado [b], A. Jorio [b],
M.A. Pimenta [b], R. Saito [c], A. Grüneis [c], G. Dresselhaus [d], M.S. Dresselhaus [e,f],
Y. Ohno [g], T. Mizutani [h], H. Shinohara [a,i,*]

[a] *CREST, Japan Science and Technology Agency c/o Department of Chemistry, Nagoya University, Chikusa-ku, Nagoya 464-8602, Japan*
[b] *Departamento de Física, Universidade Federal de Minas Gerais, Caixa Postal 702, Belo Horizonte, MG 30123-970, Brazil*
[c] *CREST, Japan Science and Technology Agency c/o Department of Physics, Tohoku University, Aoba-ku, Sendai 980-8578, Japan*
[d] *Francis Bitter Magnet Laboratory, Massachusetts Institute of Technology, Cambridge, MA 02139-4307, USA*
[e] *Department of Electrical-Engineering and Computer Science, Massachusetts Institute of Technology, Cambridge, MA 02139-4307, USA*
[f] *Department of Physics, Massachusetts Institute of Technology, Cambridge, MA 02139-4307, USA*
[g] *PRESTO, Japan Science and Technology Agency c/o Department of Quantum Engineering, Nagoya University, Chikusa-ku, Nagoya 464-8603, Japan*
[h] *Department of Quantum Engineering, Nagoya University, Chikusa-ku, Nagoya 464-8603, Japan*
[i] *Institute for Advanced Research, Nagoya University, Chikusa-ku, Nagoya 464-8602, Japan*

Received 4 June 2004; accepted 23 November 2004

Abstract

The second order Raman signals around the G'-band region of graphite and carbon nanotubes have been investigated at more than 15 excitation laser lines. Two distinct Raman bands have been observed around 2700 cm^{-1}; a prominent one is due to the so-called G'-band and the other is a weak band around 2450 cm^{-1}. Both two bands can be from the double resonance process involving two phonons around the K-point in the phonon dispersion of a two-dimensional graphite. The 2450 cm^{-1}-band has exhibited little power dependence, whereas the intensity of G'-band has shown large photon energy dependence as already reported. The 2450 cm^{-1}-band and the G'-band correspond to non-dispersive $q = 0$ and fully-dispersive $q = 2k$, respectively. From the phonon dispersion and the corresponding phonon frequency, the 2450 cm^{-1}-band can be assigned as an overtone mode of LO phonon (i.e. 2LO). This is revealed by calculated Raman spectra of graphite with proper electron–phonon matrix elements. The present study is the first report on the origin and assignment of the 2450 cm^{-1}-band, which is based on the double resonance Raman scattering.
© 2004 Elsevier Ltd. All rights reserved.

Keywords: Carbon nanotubes; Arc discharge; Raman spectroscopy; Phonons

1. Introduction

The second order Raman spectra are relatively weak and broad compared to the first order Raman spectra in the solid state, since the scattering process is possible over the whole equi-energy surface for optical absorption. Many researchers, however, reported relatively strong peaks in the second order frequency region (under 3200 cm^{-1}) in graphite [1–6] and carbon nanotubes (CNTs) [7,8]. The double resonance Raman scattering process is the most reliable explanation on the observed strong peak beyond expectation [9–11].

Here, we have investigated the second order Raman spectra of HOPG, an isolated single-wall carbon

---

nanotube (SWNT) and an isolated double-wall carbon nanotube (DWNT) around 2700 cm^{-1}, which corresponds to the phonons near the K-points. We have succeeded in assigning the Raman peak around 2450 cm^{-1} based on the double resonance scattering.

A strong peak around 2700 cm^{-1} is known as the G'-band in graphite [1–6] and CNTs [7,8], which corresponds to the overtone mode of the D-band. The origin of the G'-band has been elucidated theoretically as a double resonance, two-phonon Raman process which is independent of the presence of defects in the crystal [9–12]. The corresponding phonon is involved in an inter-valley scattering process of in-plane optical phonon modes (LO or TO) around the K-points in the two-dimensional (2D) Brillouin zone (BZ) [13]. Such optical phonon modes have large dispersion near the K-points [13], which is revealed by their dispersive nature of phonon-frequency as a function of excitation laser energy [8]. The phonon dispersion relation around the K-points can be obtained from the G'-band Raman spectra.

Some of the weak features in the second order region still have been inexplicable, although five bands have been successfully assigned (M, iTOLA, G', 2iTO, and 2G) to date [14,15]. The presence of the 2450 cm^{-1}-band in graphite related materials have been pointed out [3,7,16,17]. The present study reveals that the 2450 cm^{-1}-band shows a characteristic excitation laser energy (E_{laser}) dependence and that the Raman band originates from the two-phonon double resonance process with $q = 0$ [18]. Furthermore, the calculated Raman spectra confirm such a non-dispersive nature of the bands. This is the first assignment and identification of the 2450 cm^{-1}-band based on the double resonance Raman measurements together with theoretical calculations.

2. Experimental

2.1. Sample preparation

Single-wall CNTs (SWNTs) [19] and double-wall CNTs (DWNTs) [20] were dispersed in 1,2-dichloroethane solvent and were ultrasonicated for 15 min. After the ultrasonication, 25 µl of the solution was dropped onto a silicon substrate with a thermally oxidized surface (100 nm) which was originally patterned with "cross" marks. The substrate was rotated on a spin-coater (Kyowariken, model K-359 S-1) at 500 rpm and 1500 rpm successively for 5 and 90 s, respectively. The density of CNTs on the substrate was visualized by using an atomic force microscope (AFM: Veeco, Dimension 3100/Nanoscope IV). Typically, the density of CNTs is 5–20 tubes per 5 µm^2. Fig. 1 shows a typical AFM image of such dispersed DWNTs.
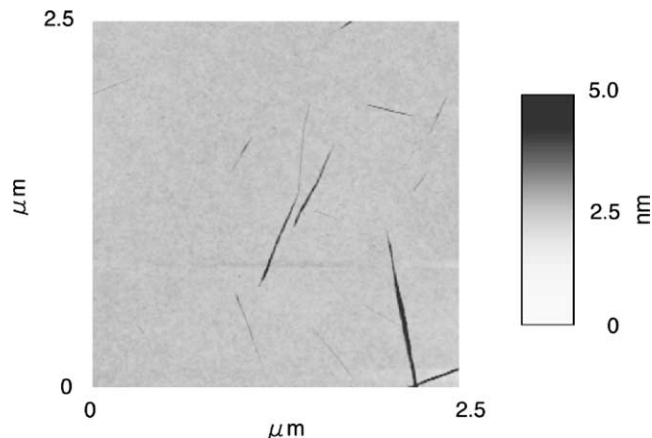

Fig. 1. A typical AFM image of isolated DWNT. In this image, the thickest bundle ($\approx$3 nm in height) contains a few DWNTs estimated by the height distribution from the AFM measurements.

2.2. Raman spectroscopy

An Ar–Kr laser (E_{laser} = 1.91–2.71 eV), a He–Ne laser (E_{laser} = 1.96 eV), and a dye-laser (E_{laser} = 1.89–1.97 eV) were employed as excitation for Raman measurements. A triple-monochromator (DILOR XY, f = 500 mm) equipped with a liquid-N$_2$ cooled charged coupled device (CCD) and a single-monochrometer (Jobin Yvon, LabRam HR800, f = 800 mm) with an air cooled CCD were used to acquire the Raman spectra. Although CNTs on the substrate were not damaged even at a high laser power, most spectra were taken with a low power density ($\approx$0.2 mW/µm^2). The "cross" marks on the substrate enabled us to obtain signals from the same position whenever the laser energy was varied.

3. Results and discussion

3.1. Raman spectra around 2700 cm^{-1}

Fig. 2 shows Raman intensity profiles for HOPG, SWNTs and DWNTs (an isolated rope and bundles) observed at E_{laser} = 2.54 eV. The spectra of HOPG and SWNTs are identical to those reported elsewhere. The G'-band principal frequency of CNTs is 50 cm^{-1} lower than that of HOPG. Although at first glance the principal peak seems to be a single peak for CNTs, in fact more than two peaks are present as revealed by a Lorentzian fitting. In view of the line width of the G'-band ($\Gamma_{G'}$) of CNTs, the spectral widths of the bundled CNTs are broader than those of the isolated one, since many (n,m) indices can be attributed to a different resonant condition. $\Gamma_{G'}$ values for DWNTs can be estimated from those for SWNTs (cf. Fig. 2). $\Gamma_{G'}$ values for both CNTs are often comparable with each other (cf. Fig. 3(a) and Fig. 4(a)).
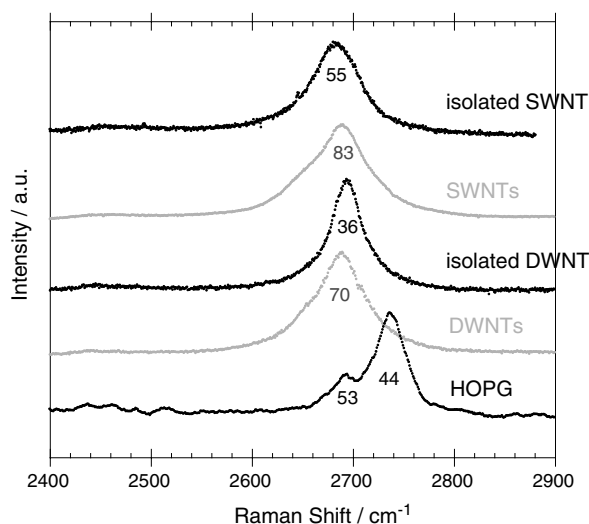
Fig. 2. G'-band spectra of isolated SWNT, bundles of SWNTs, isolated DWNT, bundles of DWNTs, and HOPG at 488 nm (2.54 eV) excitation. The line widths of the principal peaks for the G'-band are displayed in cm^{-1}.

3.2. Dispersion of second order Raman peaks

The G'-band Raman spectra from an isolated SWNT and an isolated DWNT are summarized in Figs. 3 and 4, respectively. Fig. 3(a) shows the G'-band Raman spectra of an isolated SWNT for different E_{laser}. The large dispersion of the G'-band, which originate from two-phonon scattering near the K-points, results in the upshift of the band position as E_{laser} increases. The value of $\Gamma_{G'}$ for an isolated SWNT is estimated to be 50–65 cm^{-1}. Weak features can be recognized around 2450 cm^{-1} irrespective of E_{laser}. Fig. 3(b) shows enlarged spectra (by 30 times) of the 2450 cm^{-1}-band at E_{laser} = 2.18, 2.47, 2.50, and 2.54 eV.

Fig. 4(a) and (b) show the G'-band and magnified spectra of the 2450 cm^{-1}-band of an isolated DWNT, respectively, at E_{laser} = 2.18, 2.47, 2.50, and 2.54 eV. Both the 2450 cm^{-1}- and the G'-band show almost the same E_{laser} dependence for SWNTs and DWNTs, whereas peak features and the value of $\Gamma_{G'}$ for the isolated DWNT (33–68 cm^{-1}) are somewhat different from those of SWNT. At 1.97 eV excitation, the major peak has a shoulder around 2600 cm^{-1} and at 2.50 eV the major peak splits into more than two shoulders. We have also obtained such a peak splitting at E_{laser} < 2.0 eV (cf. Fig. 5). This is due to the fact that more than one (n, m) indices of a DWNT (e.g. inner and outer) are resonant with E_{laser} at the same time. Even in an isolated DWNT, there are many possible combinations of chiral indices. Pfeiffer et al. pointed out that the G'-band (the D^*-band noted in their report) of DWNT may show a well separated double peak structure, where the low and high frequency peaks originate from the inner and outer tubes, respectively [21]. We also suggest that such
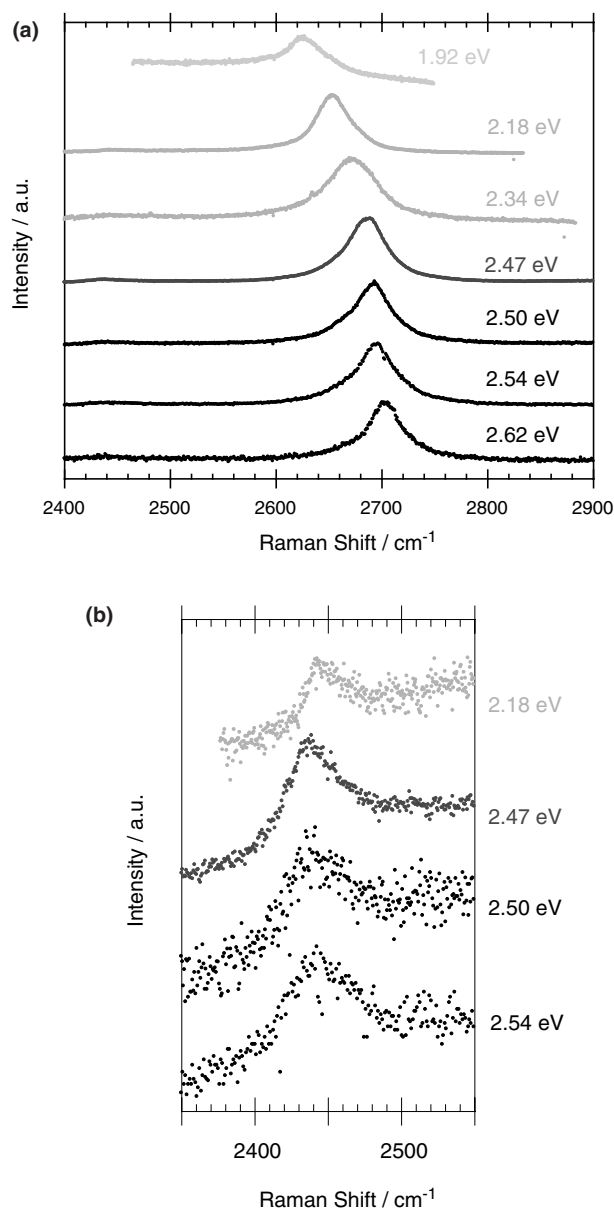

Fig. 3. (a) The G'-band spectra of isolated SWNT at 1.92, 2.18, 2.34, 2.47, 2.50, 2.54, and 2.62 eV laser energy. (b) Magnified spectra (30 times) of (a) around 2450 cm^{-1} obtained at 2.18, 2.47, 2.50, and 2.54 eV laser energy.

anomalous G'-band peaks originate from trigonal warping effect, which was already reported for an isolated SWNT in recent studies [13,22,23].

Since the weak 2450 cm^{-1}-bands have no or very small dispersion irrespective of E_{laser} we can assign the band as "$q = 0$" branch of double resonance Raman scattering as discussed in graphite [18]. Fig. 5 shows E_{laser} dependence on the Raman frequency for the 2450 cm^{-1}- and the G'-bands of HOPG, SWNT, and DWNT. The 2450 cm^{-1}-bands show almost no dispersion, whereas the salient G'-bands show a highly dispersive behavior. The dispersion of the 2450 cm^{-1}-bands
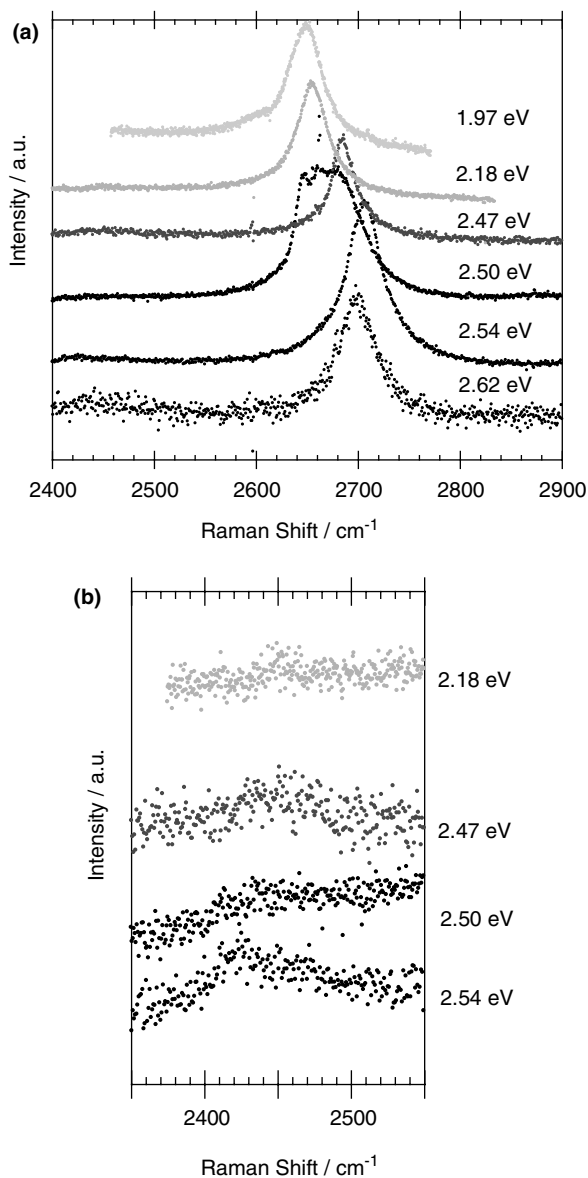
Fig. 4. (a) The G'-band spectra of isolated DWNT obtained at 1.97, 2.18, 2.47, 2.50, 2.54, and 2.62 eV excitation. (b) Magnified spectra (30 times) of (a) around 2450 cm^{-1} at 2.18, 2.47, 2.50, and 2.54 eV laser energy.
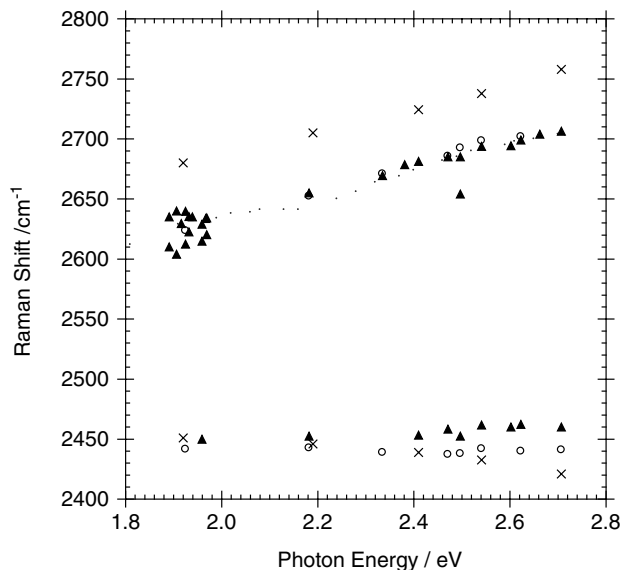

Fig. 5. G' Raman shifts dependence on the excitation laser energy for an isolated SWNT (open circle), an isolated DWNT (solid up triangle) and HOPG (cross) together with the other experimental results on SWNT (tiny dot) taken from Ref. [8].

are ∼5, ∼3, and ∼−5 cm^{-1}eV^{-1} for SWNT, DWNT and HOPG, respectively.

Kawashima and Katagiri assigned the 2446 cm^{-1}-band as combination of the 1083 cm^{-1}- and the 1357 cm^{-1}-bands because of the dispersion "0.19 cm^{-1}nm^{-1}" based on the measurement by using three laser lines [24]. Tan et al. also assigned the 2450 cm^{-1}-band as D (1350 cm^{-1}) + D'' (1090 cm^{-1}) [25–27] in reference to the study by Kawashima and Katagiri [24]. We think, however, that the 2450 cm^{-1}-band cannot be due to a combination of two types of phonon modes. If the 2450 cm^{-1}-band originates from overtone of a single phonon mode, the corresponding frequency should exist near K-points in phonon dispersion of graphite. How-

ever, a phonon at the K-points can choose momentum arbitrary, and such phonons have singularity at $q = 0$ and $2k$. In the two-phonon double scattering process, the dispersion nature should be emphasized by phonon momentum [14,15,18]. For example, the 2900 cm^{-1}-band comes from an overtone mode of iTO mode with $q = 0$ (i.e. 2iTO) [14,15], whereas the G'-band can be explained by $q = 2k$, which results in fully dispersive behavior.

3.3. Theoretical considerations on the Raman spectra

To identify and characterize the 2450 cm^{-1}-band, we have calculated resonance Raman intensity of two-dimensional graphite within tight-binding method. The electron–phonon matrix element is calculated as an inner product of phonon eigenvectors for each phonon mode and the deformation potential vector [28]. The Raman intensity of two-phonon, second-order process [15], is calculated for possible combinations of two-phonon modes around the K-point in the two-dimensional Brillouin zone. For evaluating the resonance Raman intensity, both electron–photon and electron–phonon matrix elements are taken into account. The detail calculated method is reported elsewhere [28].

Fig. 6 shows a comparison between the experimental Raman spectra of HOPG and calculated spectra for two-dimensional graphite. The maximum intensity in the calculation is normalized to the experimental peak height. The dispersive behavior of the G'-band peak around 2700 cm^{-1} and non-dispersive behavior of the peak around 2450 cm^{-1} in the experiment are clearly reproduced by the present theoretical calculation. At
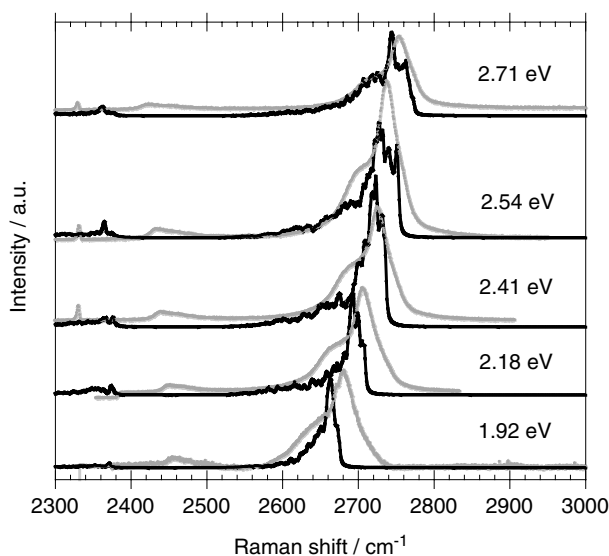
Fig. 6. Comparison between the observed Raman spectra (gray) and the corresponding calculated spectra (black) of graphite at five different excitation laser energies.

energy. Nevertheless, the present experimental data for SWNT and DWNT often show the 2450 cm^{-1} feature. This means that we can get Raman signals even at not-strict resonance condition if we simply take a sufficiently long duration time (typically 180 s, more than three times accumulation). The resonance condition is obtained at general k-points at equi-energy contour surface, which are not always close to a single vHS. In fact, the number of observed Raman peaks for an isolated CNT is much smaller than that for the bundled CNTs because we did not obtain the good resonance conditions for the limited number of SWNTs. Since the scattering process in a SWNT is the same as that in graphite, the observed 2450 cm^{-1} peaks in SWNT are assigned as $q = 0$, 2LO phonon second order scattering based on the discussion for the graphite. In the future, for known (n,m) SWNTs, resonance Raman spectra will be observed by changing the laser energy, which will give a definite answer for the assignment.

4. Conclusion

We have investigated the G' Raman spectra of HOPG, an isolated SWNT and an isolated DWNT. High quality CNT samples enable us to observe fine structure of both the G'-band and the 2450 cm^{-1}-band. The 2450 cm^{-1}-band does not show any dispersion, whereas the peak position of the G'-band is highly dependent on E_{laser} even though the corresponding phonons of both Raman bands are related with each other at steep slopes near the K-point. The observed difference can be explained consistently by the phonon dispersion occurring in the double resonance process, where non-dispersive and full-dispersive characteristics stem from $q = 0$ and $q = 2k$, respectively. The calculated energy positions of the G'-band and the 2450 cm^{-1}-band are consistent with the present observation. Further investigations on chilarity dependent double resonance studies will be needed for a more precise assignment of the Raman peaks observed in SWNTs and DWNTs.

2.54 eV, the calculated peak feature and position agree well with the experimental results, especially for the G'-band frequency. The shape and position of the 2450 cm^{-1} peaks, however, do not fully agree between experiment and calculation. The calculated Raman shift gives 100 cm^{-1} smaller for the 2450 cm^{-1} mode than the observed one. This is due to the fact that the used force constant set is not suitable for reproducing this phonon frequency at K-point. Phonon dispersion around K-point is not well established yet, though there are many important progress for phonon dispersion of graphite [29,30]. So far we use the force constant set which reasonably reproduces the one-phonon second order Raman signals [10].

Moreover, the origin of the 2450 cm^{-1} feature can be assigned to (1) $q = 0$, 2LO phonon, or (2) $q = 0$, a combination of LO and TA, (3) $q = k$, combination mode TO and LA [9,10,13,15]. These phonon modes have non-zero matrix element for these q values. Case (2) can be removed since we did not find one-phonon second order signal of TA phonon modes. We expect some dispersion behavior for case (3) and thus case (3) does not fit to the experimental values. Thus 2450 cm^{-1}-band can be tentatively assigned to case (1) characterized as overtone modes of LO phonon near the K-points. We are now investigating the origin of G'-band more systematically, which will be reported in the near future.

The G'-band spectra of a SWNT should be similar to that of graphite. A different point is that the resonance condition at van Hove singular (vHS) k-point gives a sharp and strong Raman peak which strongly depends on the laser energy. Thus the calculated relative intensity at 2450 cm^{-1} would not be well compared with the experiment if we do not know (n,m) value and resonance

References

[1] Nemanich RJ, Solin SA. Observation of an anomalously sharp feature in the 2nd order Raman spectrum of graphite. Solid State Commun 1977;23(7):417–20.

[2] Vidano RP, Fischbach R. New lines in the Raman spectra of carbons and graphite. J Am Ceram Soc 1978;61(1–2):13–7.

[3] Nemanich RJ, Solin SA. First- and second-order Raman scattering from finite-size crystals of graphite. Phys Rev B 1979; 20(2):392–401.

[4] Vidano RP, Fischbach DB, Willis LJ, Loehrv TM. Observation of Raman band shifting with excitation wavelength for carbons and graphites. Solid State Commun 1981;39(2):341–4.

[5] Al-Jishi R, Dresselhaus G. Lattice-dynamical model for graphite. Phys Rev B 1982;26(8):4514–22.

[6] Al-Jishi R, Dresselhaus G. Lattice-dynamical model for alkali–metal–graphite intercalaion compounds. Phys Rev B 1982;26(8): 4523–38.

[7] Kastner J, Pichler T, Kuzmany H, Curran S, Blau W, Weldon DN, et al. Resonance Raman and infrared spectroscopy of carbon nanotubes. Chem Phys Lett 1994;221(1-2):53–8.

[8] Pimenta MA, Hanlon EB, Marucci A, Corio P, Brown SDM, Empedocles SA, et al. The anomalous dispersion of the disorder-induced and the second-order Raman bands in carbon nanotubes. Braz J Phys 2000;30(2):423–7.

[9] Saito R, Jorio A, Souza Filho AG, Dresselhaus G, Dresselhaus MS, Pimenta MA. Probing phonon dispersion relations of graphite by double resonance Raman scattering. Phys Rev Lett 2002;88(2):027401-1–4.

[10] Grüneis A, Saito R, Kimura T, Cançado LG, Pimenta MA, Jorio A, et al. Determination of two-dimensional phonon dispersion relation of graphite by Raman spectroscopy. Phys Rev B 2002; 65(15):155405-1–7.

[11] Kürti J, Zólyomi V, Grüneis A, Kuzmany H. Double resonant Raman phenomena enhanced by van Hove singularities in single-wall carbon nanotubes. Phys Rev B 2002;65(16):165433-1–9.

[12] Dresselhaus MS, Dresselhaus G, Jorio A, Souza Filho AG, Saito R. Raman spectroscopy on isolated single wall carbon nanotubes. Carbon 2002;40(12):2043–61.

[13] Samsonidze GG, Saito R, Jorio A, Souza Filho AG, Grüneis A, Pimenta MA. Phonon trigonal warping effect in graphite and carbon nanotubes. Phys Rev Lett 200;90(2):027403-1–4.

[14] Brar VW, Samsonidze GG, Dresselhaus MS, Dresselhaus G, Saito R, Swan AK, et al. Second-order harmonic and combination modes in graphite, single-wall carbon nanotube bundles, and isolated single-wall carbon nanotubes. Phys Rev B 2002;66(15):155418-1–10.

[15] Saito R, Grüneis A, Samsonidze GG, Brar VW, Dresselhaus G, Dresselhaus MS, et al. Double resonance Raman spectroscopy of single-wall carbon nanotubes. New J Phys 2003;5. Article 157.

[16] Wright RB, Varma R, Gruen DM. Raman scattering and SEM studies of graphite and silicon carbide surfaces bombarded with energetic protons, deutrons and helium ions. J Nucl Mater 1976;63(1):415–21.

[17] Elman BS, Dresselhaus MS, Dresselhaus G, Maby EW, Mazurek H. Raman scattering from ion-implanted graphite. Phys Rev B 1981;24(2):1027–34.

[18] Cançado LG, Pimenta MA, Saito R, Jorio A, Ladeira LO, Grüeneis A, et al. Stokes- and anti-Stokes double resonance Raman scattering in two-dimensional graphite. Phys Rev B 2002; 66(3):035415-1–5.

[19] Shimada T, Ohno Y, Okazaki T, Sugai T, Suenaga K, Iwatsuki S, et al. Transport properties of C_{78}, C_{90} and $Dy@C_{82}$ fullerenes-nanopeapods by field effect tramsistors. Physica E 2004;21(2–4): 1089–92.

[20] Sugai T, Yoshida H, Shimada T, Okazaki T, Shinohara H, Bandow S. New synthesis of high-quality double-walled carbon nanotubes by high temperature pulsed arc discharge. Nano Lett 2003;3(6):769–73.

[21] Pfeiffer R, Simon F, Hulman M, Kramberger Ch, Lolzweber M, Kuzmany H, et al. The inside of SWCNTS: a clean room reactor for nano phases. Abstract of XVII Int'l. Winterschool/Euroconference on Electronic Properties of Novel Materials, 2004.

[22] Souza Filho AG, Jorio A, Samsonidze GG, Dresselhaus G, Dresselhaus MS, et al. Probing the electronic trigonal warping effect in individual single-wall carbon nanotubes using phonon spectra. Chem Phys Lett 2002;354(1-2):62–8.

[23] Souza Filho AG, Jorio A, Swan AK, Ünlü MS, Goldberg BB, Saito R, et al. Anomalous two-peak G'-band Raman effect in one isolated single-wall carbon nanotube. Phys Rev B 2002;65(8): 085417-1–8.

[24] Kawashima Y, Katagiri G. Fundamentals, overtones, and combinations in the Raman spectrum of graphite. Phys Rev B 1995; 52(14):10053–8.

[25] Tan PH, Deng YM, Zhao Q. Temperature-dependent Raman spectra and anomalous Raman phenomenon of high oriented pyrolytic graphite. Phys Rev B 1998;58(9):5435–9.

[26] Tan PH, Hu CY, Dong J, Shen WC, Zhang BF. Polarization properties, high-order Raman spectra, and frequency asymmetry between Stokes and anti-Stokes scattering of Raman modes in a graphite. Phys Rev B 2001;64(21):214301-1–12.

[27] Tan PH, An L, Liu LQ, Guo ZX, Czerw R, Carroll DL, et al. Probing the phonon dispersion relations of graphite from the double-resonance process of Stokes and anti-Stokes Raman scatterings in multiwalled carbon nanotubes. Phys Rev B 2002; 66(24):245410-1–8.

[28] Gruneis A. Thesis. Tohoku University, 2004.

[29] Maultzsch J, Reich S, Thomsen C, Requardt H, Ordejón R. Phonon dispersion in graphite. Phys Rev Lett 2004;92(7):075501-1–4.

[30] Wirtz L, Rubio A. The phonon dispersion of graphite revisited. Solid State Commun 2004;131(3-4):141–52.